

Effect of Adsorption on the Surface Tensions of Solid–Fluid Interfaces

C. A. Ward* and Jiyu Wu

Thermodynamics and Kinetics Laboratory, Department of Mechanical and Industrial Engineering, University of Toronto, Toronto, Canada M5S 3G8

Received: October 27, 2006; In Final Form: January 30, 2007

A method is proposed for determining the surface tensions of a solid in contact with either a liquid or a vapor. Only an equilibrium adsorption isotherm at the solid–vapor interface needs to be added to Gibbsian thermodynamics to obtain the expressions for the solid–vapor and the solid–liquid surface tensions, $\gamma_{[1]}^{SV}$ and $\gamma_{[1]}^{SL}$, respectively. An equilibrium adsorption isotherm relation is formulated that has the essential property of *not* predicting an infinite amount adsorbed when the pressure is equal to the saturation-vapor pressure. Five different solid–vapor systems from the literature are examined, and found to be well described by the new isotherm relation. The surface-tension expressions obtained from the isotherm relation are examined by determining the surface tension of the solid in the absence of adsorption, $\gamma_{[1]}^{S0}$, a material property of a solid surface. The value of $\gamma_{[1]}^{S0}$ can be determined by adsorbing different vapors on the same solid, determining the isotherm parameters in each case, and then from the expression for $\gamma_{[1]}^{SV}$ taking the limit of the pressure vanishing to determine $\gamma_{[1]}^{S0}$. From previously reported measurements of benzene and of *n*-hexane adsorbing on graphitized carbon, the same value of $\gamma_{[1]}^{S0}$ is obtained.

1. Introduction

The surface tensions of a solid surface contacting a vapor, γ^{SV} , or a liquid, γ^{SL} , cannot be measured directly, but must be inferred. These surface tensions are related to the contact angle, θ , through the well-established Young equation:^{1–3}

$$\gamma^{SV} - \gamma^{SL} = \gamma^{LV} \cos \theta \quad (1)$$

The methods proposed to infer the values of γ^{SV} and γ^{SL} generally accept the Young equation, but another relation is required. It has been supposed that the additional relation requires the introduction of a new postulate or hypothesis that is outside thermodynamics.⁴ Chibowski and Perea-Carpio reviewed several of these hypotheses, pointing out that none allows an “unambiguous interpretation of the experimental data ...”.⁵

We propose a new method for inferring the values of γ^{SV} and γ^{SL} in which only an adsorption isotherm at the solid–vapor interface is added to Gibbsian thermodynamics.¹ The positions of the interfaces at the solid–vapor and solid–liquid interfaces are chosen to be such that there is no adsorption of the solid component. Adsorption from the fluid phases is fully taken into account. The Gibbs adsorption equations and the necessary conditions for equilibrium are applied to show that if the pressure is such that θ can exist, the adsorption at the solid–liquid interface, $n_{[1]}^{SL}$, can be expressed in terms of θ and the adsorption isotherm at the solid–vapor interface, $n_{[1]}^{SV}$. The bracketed subscript indicates the choice of the interface position. For the isothermal system considered, the independent variable of θ , $\gamma_{[1]}^{SV}$ and $\gamma_{[1]}^{SL}$, is shown to be the ratio of the liquid-phase pressure at the three-phase line, $P^L(z_3)$, to the saturation-vapor pressure, $P_s(T)$, denoted as x_3^L , where the subscript 3 indicates it is evaluated at the three-phase line. This greatly simplifies

the formulation, and allows $\gamma_{[1]}^{SV}$ and $\gamma_{[1]}^{SL}$, relative to a reference state, to be expressed in terms of an integral of $n_{[1]}^{SV}$. However, isotherms which indicate an infinite amount adsorbed when the pressure is equal the saturation-vapor pressure cannot be applied because the integral does not converge.

An adsorption isotherm relation, called the ζ -isotherm, is developed by approximating the adsorbed vapor as molecular clusters adsorbed at sites, as suggested by the observations of Frazer.⁶ The ζ -isotherm reduces to the Anderson isotherm⁷ in a particular limit, and is examined experimentally for pressures from near zero to near the saturation vapor pressure by using data from the literature. Five systems are considered: benzene and *n*-hexane adsorbing on graphitized carbon,⁸ H₂O adsorbing on silica (TK800) and on alumina (Baikowski CR1);⁹ and benzene adsorbing on pulverized quartz.¹⁰ For each system, the parameters appearing in the ζ -isotherm are determined. Although for each system considered the calculations are in good-to-excellent agreement with the measurements, the ζ -isotherm does not indicate an infinite adsorption at the saturation pressure for any of the systems considered.

When the pressure is too small to allow θ to exist, the ζ -isotherm is used to construct the expression for $\gamma_{[1]}^{SV}$ as a function of the ratio vapor-phase pressure to $P_s(T)$, denoted x^V . This allows the proposed theory to be subjected to an important test. When $\gamma_{[1]}^{SV}$ is evaluated at $x^V = 0$, a material property of the solid surface is obtained, $\gamma_{[1]}^{S0}$. But it is expressed in terms of γ^{LV} and the adsorption parameters. Since the adsorption of benzene and *n*-hexane on the same substrate, graphitized carbon, has been previously measured, the value of $\gamma_{[1]}^{S0}$ for graphitized carbon can be determined from these two independent sets of measurements. We find the two values of $\gamma_{[1]}^{S0}$, obtained from benzene and *n*-hexane measurements, are not measurably different. A similar test is provided by quartz and silica (TK800). Although the surface of these materials is polycrystalline, they consist of primarily of SiO₂, and thus would be expected to

* Address correspondence to this author. E-mail: ward@mie.utoronto.ca.

have similar values of $\gamma_{[1]}^{SO}$. We find the mean values of their surface tensions differ by 8%.

2. Expressions for $\gamma_{[1]}^{SV}$ and $\gamma_{[1]}^{SL}$ When the Pressure Is Such That the Contact Angle Can Exist

Consider a single component fluid filling a cylinder that is maintained at temperature T . Depending on the pressure, the system can adopt different configurations. We first suppose the pressure is such that the liquid and vapor phases are present, and at the line formed where they contact the solid surface at height z_3 , an equilibrium contact angle, θ , is formed. The maximum value that θ can have is π , and the minimum is zero. The pressure ratios in the liquid phase at the three-phase line when the contact angle has these values are denoted x_w^L and x_π^L , respectively. Second, when the pressure ratio is below x_w^L the contact angle cannot exist, but equilibrium between the vapor and adsorbed phase can.

2.1. The Independent Variable for an Isothermal Three-Phase System. For an equilibrium contact angle to exist in the system, the pressure ratio must be in the range

$$x_w^L \leq x_3^L \leq x_\pi^L \quad (2)$$

and the chemical potentials of the molecules in phase j , μ^j , must satisfy

$$\mu^{SV} = \mu^{SL}; \quad \mu^{SL} = \mu^L; \quad \mu^L = \mu^V \quad (3)$$

where SV , SL , L , and V denote the solid–vapor, solid–liquid, liquid, and vapor phases, respectively. If we assume the liquid phase may be approximated as incompressible

$$\mu^L(T, x^L) = \mu(T, P_s) + v_f P_s (x^L - 1) \quad (4)$$

where T is the temperature, and v_f is the specific volume of the saturated liquid at T . The Gibbs adsorption equations at the solid–liquid interface may be written

$$d\gamma_{[1]}^{SL} = -n_{[1]}^{SL} d\mu^{SL} \quad (5)$$

and at the solid–vapor interface

$$d\gamma_{[1]}^{SV} = -n_{[1]}^{SV} d\mu^{SV} \quad (6)$$

After taking the differential of eqs 3 and 4 and applying the result at the three-phase line, one finds eq 5 may be written

$$d\gamma_{[1]}^{SL} = -n_{[1]}^{SL} v_f P_s dx_3^L \quad (7)$$

and similarly, eq 6 becomes

$$d\gamma_{[1]}^{SV} = -n_{[1]}^{SV} v_f P_s dx_3^L \quad (8)$$

Equations 7 and 8 indicate that, for the isothermal system we consider, $\gamma_{[1]}^{SV}$ and $\gamma_{[1]}^{SL}$ each has x_3^L as its independent variable. And then, from eq 1, θ does as well:

$$\theta = \theta(x_3^L) \quad (9)$$

After taking the differential of eq 1, and combining with eqs 7 and 8, one finds

$$n_{[1]}^{SL}(x_3^L) = n_{[1]}^{SV}(x_3^L) + \frac{\gamma^{LV}}{v_f P_s} \left[\frac{d \cos \theta(x_3^L)}{dx_3^L} \right] \quad (10)$$

The expression for $n_{[1]}^{SL}(x_3^L)$ given in eq 10 may be substituted into eq 7, and the result integrated. To choose the limits of the integral, we note that if the vapor is approximated as an ideal gas, then

$$\mu^V(T, P^V) = \mu(T, P_s) + k_b T \ln(x^V) \quad (11)$$

where k_b denotes the Boltzmann constant. If v_g denotes the specific volume of the saturated vapor at T , one finds from eqs 3, 4, and 11 that at the three-phase line

$$x_3^V = \exp \left[\frac{v_f}{v_g} (x_3^L - 1) \right] \quad (12)$$

Thus, either x_3^L or x_3^V may be chosen as the independent variable for θ , $\gamma_{[1]}^{SV}$, and $\gamma_{[1]}^{SL}$. Also, as seen from eq 12, if x_3^L has a value of unity, then so does x_3^V . For the pressures in the liquid and vapor phases to have the same value, the liquid–vapor interface cannot have any curvature, or in other words, the contact angle must be $\pi/2$; thus,

$$\cos \theta(1) = 0 \quad (13)$$

If x_3^L is set equal to unity in eq 1, then it is found that $\gamma_{[1]}^{SV}(1)$ and $\gamma_{[1]}^{SL}(1)$ are equal, and we denote their value as γ_\perp . Hence, if eq 10 is substituted into eq 7, and the result integrated:

$$\gamma_{[1]}^{SL}(x_3^L) - \gamma_\perp = - \int_1^{x_3^L} n_{[1]}^{SV}(x_d^L) v_f P_s dx_d^L - \gamma^{LV} \cos \theta(x_3^L) \quad (14)$$

and integrating eq 8 between the same limits gives

$$\gamma_{[1]}^{SV}(x_3^L) - \gamma_\perp = - \int_1^{x_3^L} n_{[1]}^{SV}(x_d^L) v_f P_s dx_d^L \quad (15)$$

If the expression for $n_{[1]}^{SV}$ were available, eqs 14 and 15 could be integrated to obtain the expressions for $\gamma_{[1]}^{SL}(x_3^L)$ and $\gamma_{[1]}^{SV}$ in terms of their independent variable, x_3^L , and the reference surface tension, γ_\perp .

2.2. The Wetting Hypothesis for Pressures Where the Contact Angle Can Exist. From thermodynamics alone, the numerical value of the surface tensions (or surface energies) cannot be obtained. We adopt the wetting hypothesis to establish a scale for solid–fluid surface tensions. The wetting hypothesis assumes that when x_3^L is equal to x_w^L , $\gamma_{[1]}^{SL}(x_w^L)$ vanishes. The consistency of the wetting hypothesis will be examined below, but we first apply it to determine the expression for γ_\perp .

If eq 14 is evaluated at x_w^L

$$\gamma_\perp = \int_1^{x_w^L} n_{[1]}^{SV}(x_d^L) v_f P_s dx_d^L + \gamma^{LV} \quad (16)$$

When the expression for γ_\perp is inserted into eq 15, one finds, after simplification

$$\gamma_{[1]}^{SV}(x_3^L) = \gamma^{LV} - I_\theta(x_w^L, x_3^L) \quad (17)$$

where $I_\theta(x_w^L, x_3^L)$ is defined as

$$I_\theta(x_w^L, x_3^L) \equiv \int_{x_w^L}^{x_3^L} n_{[1]}^{SV}(x_d^L) v_f P_s dx_d^L \quad (18)$$

When x_3^L is equal to x_w^L , the integral $I_\theta(x_w^L, x_3^L)$ vanishes, and one finds from eq 17

$$\gamma_{[1]}^{SV}(x_w^L) = \gamma^{LV} \quad (19)$$

The result given in eq 19 could also have been obtained by evaluating the Young equation at x_3^L equal x_w^L and applying the wetting hypothesis. Also, $\gamma_{[1]}^{SL}(x_3^L)$ may be written in terms of $I_\theta(x_w^L, x_3^L)$: if eq 16 is inserted into eq 14 and the result simplified

$$\gamma_{[1]}^{SL}(x_3^L) = \gamma^{LV}[1 - \cos \theta(x_3^L)] - I_\theta(x_w^L, x_3^L) \quad (20)$$

Below, we examine the magnitude of $I_\theta(x_w^L, x_3^L)$ compared with γ^{LV} . This requires the value of x_w^L and the expression for $n_{[1]}^{SV}(x_3^L)$ to be known.

2.3. Expression for the Adsorption Isotherm at the Solid–Vapor Interface. When θ exists in a system, x_3^L and x_3^V are near unity, but at present, there is no adsorption isotherm that has been proven experimentally valid in the limit of x_3^V approaching unity. The BET,¹¹ FHH,^{12–14} and AD¹⁵ isotherms all indicate $n_{[1]}^{SV}$ approaches infinity in this limit. Anderson⁷ pointed out that better agreement with experimental data was obtained if x^V in the BET isotherm expression were multiplied by a constant that was less than unity and varied from one system to another. With this modification of the BET isotherm, the expression for $n_{[1]}^{SV}$ becomes

$$n_{[1]}^{SV} = \frac{M c \alpha x^V}{(1 - \alpha x^V)[1 + (c - 1)\alpha x^V]} \quad (21)$$

where M denotes the number of adsorption sites per unit area of the solid surface, α the Anderson parameter, and c a temperature-dependent parameter. When the Anderson correction is introduced, the adsorption is no longer predicted to be infinite in the limit of x_3^V approaching unity. We investigate the theoretical basis for the Anderson correction.

Hill introduced a model of an adsorbate that he later called “physically unrealistic” in which the adsorbed molecules were assumed to assemble at the adsorption sites in non-interacting, vertical stacks with an arbitrary number in each stack.¹⁶ Using the grand canonical ensemble, he was able to obtain eq 21 and to give a molecular interpretation of the BET equation, but he ignored Anderson’s earlier empirical observation, and took α in eq 21 to have a value of unity. This reduces eq 21 to the BET equation.

Earlier, Frazer⁶ had used ellipsometry to observe water adsorption on glass and noted that as x^V approached unity, molecular clusters formed at the adsorption sites. We develop an adsorption isotherm expression that incorporates Frazer’s observations in the model of the adsorbate. At the solid–vapor interface, we suppose there are M adsorption sites per unit area, that as many as ζ molecules may adsorb in a molecular cluster at one site, and we treat each cluster of k molecules as a chemical species, and each cluster is approximated as a three-dimensional, quantum mechanical, harmonic oscillator having a fundamental frequency that depends on the number of molecules in the cluster, $\omega^{(k)}$. We neglect the internal degrees of freedom of a cluster and approximate each cluster as a mass of $k \times m$, where m is the mass of a vapor molecule. If $\epsilon_0^{(k)}$ is the zero-point energy of each degree of freedom of a cluster of k molecules, and \hbar denotes the Planck constant divided by 2π , then the energy levels of each degree of freedom of a cluster may be written

$$\epsilon_j^{(k)} = \epsilon_0^{(k)} + j\hbar\omega^{(k)} \quad j = 0, 1, 2, \dots; \quad k = 1, 2, 3, \dots, \zeta \quad (22)$$

If a_k denotes the total number of type k clusters on the surface, and if the total surface area is A , then

$$A n_{[1]}^{SV} = \sum_{k=1}^{\zeta} k a_k \quad (23)$$

If the number of empty adsorption sites is denoted as a_0 , then

$$AM = a_0 + \sum_{k=1}^{\zeta} a_k \quad (24)$$

The total energy, E , of the adsorbed molecules may be expressed in terms of a_k and the number of phonons of each type, I_k :

$$E(a_1, a_2, \dots, a_\zeta, I_1, I_2, \dots, I_\zeta) = \sum_{k=1}^{\zeta} (3a_k \epsilon_0^{(k)} + I_k \hbar \omega^{(k)}) \quad (25)$$

The energy degeneracy, g_e , of the type k phonons is the number of ways the phonons of this type may be distributed over the a_k molecular clusters:

$$g_e = \frac{(3a_k + I_k - 1)!}{(3a_k - 1)!(I_k!)} \quad (26)$$

and the configurational degeneracy, g_c , is the number of ways the clusters may be distributed over the adsorption sites with at most one cluster per site:

$$g_c = \frac{(AM)!}{\zeta \prod_{k=1}^{\zeta} a_k!} \quad (27)$$

The canonical partition function for the adsorbate viewed as ζ different adsorbed species is found to be

$$Q = g_c \prod_{k=1}^{\zeta} (q_k)^{a_k} \quad (28)$$

where

$$q_k = \left(\frac{\exp\left[\frac{-\epsilon_0^{(k)}}{k_b T}\right]}{1 - \exp\left[\frac{-\hbar\omega^{(k)}}{k_b T}\right]} \right)^3 \quad (29)$$

We suppose the partition function for a type k cluster may be written as a product:

$$q_k = q_1(q_v)^{k-1}; \quad k = 2, 3, \dots, \zeta \quad (30)$$

Note that q_k is a function of temperature, but of no other thermodynamic properties.

From the relation between the Helmholtz function and the canonical partition function, the chemical potential expression of the adsorbed clusters containing k molecules may be found by differentiating the partition function with respect to a_k :

$$\mu_k = k_b T \ln \left(\frac{a_k}{a_0 q_k} \right) \quad (31)$$

Under equilibrium conditions between clusters consisting of k molecules and the clusters containing only one molecule

$$\mu_k = k \mu_1 \quad (32)$$

and between the single-molecule clusters and the molecules in the vapor phase

$$\mu_1 = \mu^V \quad (33)$$

From eqs 31 and 32

$$\frac{a_k}{a_1} = \frac{q_k}{q_1} \exp\left[\frac{(\mu_k - \mu_1)}{k_b T}\right] \quad (34)$$

Since the vapor phase has been approximated as an ideal gas, one finds from eqs 11, 30, 32, 33, and 34 that

$$\frac{a_k}{a_1} = (\alpha x^V)^{k-1} \quad (35)$$

where

$$\alpha \equiv q_v \exp\left[\frac{\mu(T, P_s)}{k_b T}\right] \quad (36)$$

Note that temperature is the only thermodynamic property that α depends on.

After eq 35 is substituted into eq 24, the series summed, and the result solved for a_0 , one finds

$$a_0 = AM - \frac{a_1[(\alpha x^V)^\zeta - 1]}{(\alpha x^V - 1)} \quad (37)$$

An expression for a_1 is obtained by first writing eq 33 as

$$k_b T \ln\left(\frac{a_1}{a_0 q_1}\right) = k_b T \ln\left(\frac{\alpha x^V}{q_v}\right) \quad (38)$$

where we have made use of eqs 31, 11, and 36; then substituting eq 37 into eq 38 and solving for a_1 :

$$a_1 = c \alpha x^V \left(AM - \frac{a_1[(\alpha x^V)^\zeta - 1]}{(\alpha x^V - 1)} \right) \quad (39)$$

where

$$c = \frac{q_1}{q_v} \quad (40)$$

A second expression for a_1 is obtained by first solving eq 35 for a_k , substituting the result into eq 23, and summing the arithmetic-geometric series:

$$\frac{A n_{[1]}^{SV}}{a_1} = \frac{[1 - (\alpha x^V)^\zeta](1 - \alpha x^V)}{(1 - \alpha x^V)^2} + \frac{\alpha x_i^V [1 - \zeta(\alpha x^V)^{\zeta-1} + (\zeta - 1)(\alpha x^V)^\zeta]}{(1 - \alpha x^V)^2} \quad (41)$$

and solving eq 41 for a_1 . After equating the expression for a_1 given in eq 41 to that in eq 39, an expression $n_{[1]}^{SV}$ is obtained.

TABLE 1: Parameters of the ζ -Isotherm for Benzene Adsorbing on Graphitized Carbon at 20 °C Obtained from the Data of Isirikyan and Kiselev⁸

| ζ | error,% | M (kmol/m ²) | c | α | $\gamma_{[1]}^{SO}$ (kg/s ²) |
|----------|---------|--|-----------------------|-----------------------|--|
| 20 | 1.19 | 3.97×10^{-9} $\pm 1.0 \times 10^{-10}$ | 114.62 ± 16.7 | 0.8510 ± 0.009 | |
| 40 | 1.07 | 3.97×10^{-9} $\pm 8.5 \times 10^{-11}$ | 115.86 ± 15.06 | 0.8472 ± 0.007 | |
| 60 | 1.07 | 3.96×10^{-9} $\pm 8.5 \times 10^{-11}$ | 115.97 ± 15.04 | 0.8473 ± 0.007 | |
| 80 | 1.07 | 3.96×10^{-9} $\pm 8.5 \times 10^{-11}$ | 115.97 ± 15.04 | 0.8473 ± 0.007 | |
| 100 | 1.07 | 3.96×10^{-9} $\pm 8.5 \times 10^{-11}$ | 115.97 ± 15.04 | 0.8473 ± 0.007 | |
| ∞ | 1.07 | 3.96×10^{-9} $\pm 8.5 \times 10^{-11}$ | 115.97 ± 15.04 | 0.8473 ± 0.007 | 0.091 ± 0.003 |

TABLE 2: Parameters of the ζ -Isotherm for *n*-Hexane Adsorbing on Graphitized Carbon at 20 °C Obtained from the Data of Isirikyan and Kiselev⁸

| ζ | error,% | M (kmol/m ²) | c | α | $\gamma_{[1]}^{SO}$ (kg/s ²) |
|----------|---------|--|-----------------------|-----------------------|--|
| 20 | 0.70 | 3.43×10^{-9} $\pm 4.1 \times 10^{-11}$ | 876.71 ± 62.32 | 0.8239 ± 0.006 | |
| 40 | 0.68 | 3.43×10^{-9} $\pm 3.9 \times 10^{-11}$ | 875.45 ± 60.03 | 0.8211 ± 0.005 | |
| 60 | 0.68 | 3.43×10^{-9} $\pm 3.9 \times 10^{-11}$ | 875.46 ± 60.02 | 0.8211 ± 0.005 | |
| 80 | 0.68 | 3.43×10^{-9} $\pm 3.9 \times 10^{-11}$ | 875.46 ± 60.02 | 0.8211 ± 0.005 | |
| 100 | 0.68 | 3.43×10^{-9} $\pm 3.9 \times 10^{-11}$ | 875.46 ± 60.02 | 0.8211 ± 0.005 | |
| ∞ | 0.68 | 3.43×10^{-9} $\pm 3.9 \times 10^{-11}$ | 875.46 ± 60.02 | 0.8211 ± 0.005 | 0.088 ± 0.001 |

After simplifying, one finds

$$n_{[1]}^{SV} = \frac{M c \alpha x^V [1 - (1 + \zeta)(\alpha x^V)^\zeta + \zeta(\alpha x^V)^{1+\zeta}]}{(1 - \alpha x^V)[1 + (c - 1)\alpha x^V - c(\alpha x^V)^{1+\zeta}]} \quad (42)$$

We refer to the expression for $n_{[1]}^{SV}$, given in eq 42, as the ζ -isotherm relation.

Hill¹⁶ obtained eq 42 at an intermediate step of his derivation of the BET isotherm, but since he had used the grand canonical ensemble, he had to take a limit in which ζ approached infinity. He implicitly assumed the product αx_i^V to be less than unity, and found that in this limit eq 42 reduced to eq 21. He then assumed α was equal to unity, which reduced his result to the BET equation. Since we have used the canonical ensemble, it is not necessary to take the limit of ζ approaching infinity. This allows us to empirically investigate the maximum number of molecules in a cluster when the adsorbed vapor is at equilibrium.

2.4. Assessment of the Adsorption Isotherm Expression.

The ζ -isotherm contains four parameters: M , c , α , and ζ . We investigate the isotherm by determining if the parameters may be selected so the measured amount adsorbed in five different systems corresponds with that calculated. The NonlinearFit package of Mathematica is used to select the values of the parameters. Because of the complexity of the isotherm expression, all four parameters could not be determined simultaneously for each of the systems considered. We proceed by assuming a value of ζ and determine the values of M , c , and α that give the best agreement with the measurements for that value of ζ . A series of different ζ values is considered for each system. The errors in the calculated amount adsorbed for a particular value of ζ , denoted $\Delta(\zeta)$, are compared and the appropriate value

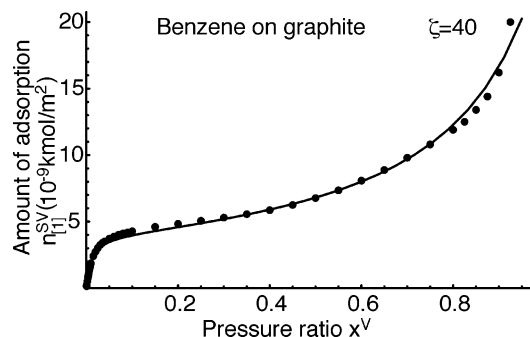


Figure 1. The solid dots indicate the measured amount of benzene adsorbed on graphitized carbon at 20 °C.⁸ The solid line is the amount calculated from the ζ -isotherm relation when the maximum number of molecules in a cluster is 40. The other parameter values are listed in Table 1.

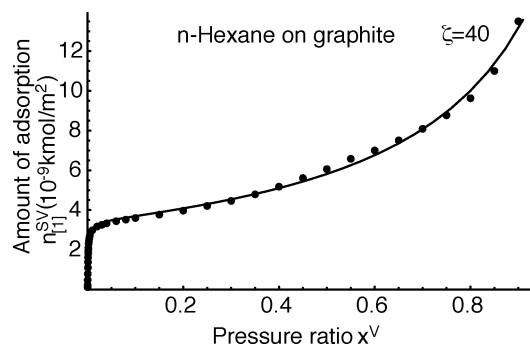


Figure 2. The solid dots indicate the measured amount of *n*-hexane adsorbed on graphitized carbon at 20 °C.⁸ The solid line is the amount calculated from the ζ -isotherm relation when the maximum number of molecules in a cluster is 40. The other parameter values are listed in Table 2.

of ζ chosen. The expression for $\Delta(\zeta)$ is

$$\Delta(\zeta) \equiv \frac{\sqrt{\sum_{j=1}^{N_m} [n_{mes}^{SV}(x_j^V) - n_{cal}^{SV}(\zeta, x_j^V)]^2}}{\sum_{j=1}^{N_m} n_{mes}^{SV}(x_j^V)} \quad (43)$$

where $n_{mes}^{SV}(x_j^V)$ is the amount measured at the relative pressure x_j^V , and $n_{cal}^{SV}(\zeta, x_j^V)$ is the amount calculated from the ζ -isotherm to be present at that value of x_j^V and the particular value of ζ . The number of measurements is denoted N_m .

Isirikyan and Kiselev⁸ studied the adsorption of benzene and *n*-hexane on graphitized carbon. Thermal carbon blacks were graphitized at 3000 ± 300 °C in the absence of air to produce a nonporous adsorbent with a homogeneous surface that was thermally and chemically stable. Electron micrographs and the X-ray diffraction measurements indicated that the initially spherical particles became polyhedra with surfaces that were mainly the homogeneous, single crystal, basal planes of graphite.^{17–19}

The adsorbed amount of benzene at 42 different values of x^V in the range from 0.0005 to 0.925 at 20 °C was measured.⁸ In Table 1, the values of the isotherm parameters corresponding to the different values of ζ are listed, along with the error in the calculations for each case. Note that provided $\zeta \geq 40$, the error, $\Delta(\zeta)$, in the calculated amount adsorbed is less than 1.1%. In Figure 1, the calculated amount adsorbed for $\zeta = 40$ is shown along with the measurements.

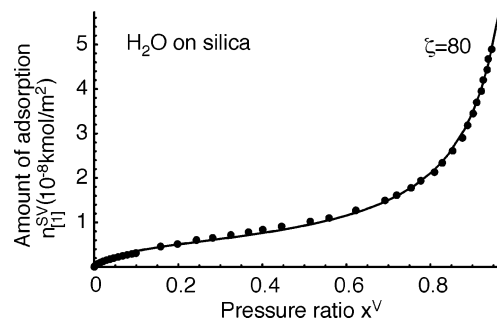


Figure 3. The solid dots indicate the measured amount of water vapor adsorbed on silica TK800 at 30 °C.⁹ The solid line is the amount calculated from the ζ -isotherm relation when the maximum number of molecules in a cluster is 80. The other parameter values are listed in Table 3.

TABLE 3: Parameters of the ζ -Isotherm for Water Vapor Adsorbing on Silica (TK800) at 30 °C Obtained from the Data of Naono and Hakuman⁹

| ζ | error,% | M (kmol/m ²) | c | α | $\gamma_{[1]}^{SO}$ (kg/s ²) |
|----------|---------|--|---------------------|------------------------|--|
| 20 | 1.81 | 5.08×10^{-9} $\pm 6.3 \times 10^{-10}$ | 12.09 ± 6.63 | 0.9980 ± 0.03 | |
| 40 | 0.67 | 5.12×10^{-9} $\pm 1.0 \times 10^{-10}$ | 16.42 ± 2.55 | 0.9522 ± 0.003 | |
| 60 | 0.56 | 5.23×10^{-9} $\pm 7.7 \times 10^{-11}$ | 15.67 ± 1.88 | 0.9456 ± 0.002 | |
| 80 | 0.54 | 5.25×10^{-9} $\pm 7.3 \times 10^{-11}$ | 15.55 ± 1.81 | 0.9448 ± 0.0019 | |
| 100 | 0.54 | 5.25×10^{-9} $\pm 7.2 \times 10^{-11}$ | 15.54 ± 1.80 | 0.9447 ± 0.0019 | |
| ∞ | 0.54 | 5.25×10^{-9} $\pm 7.2 \times 10^{-11}$ | 15.54 ± 1.79 | 0.9447 ± 0.0019 | 0.145 ± 0.003 |

TABLE 4: Parameters of the ζ -Isotherm for Water Vapor Adsorbing on Alumina (Baikowski CR1) at 20 °C Obtained from the Data of Naono and Hakuman⁹

| ζ | error,% | M (kmol/m ²) | c | α | $\gamma_{[1]}^{SO}$ (kg/s ²) |
|----------|---------|--|----------------------|------------------------|--|
| 20 | 1.19 | 1.03×10^{-8} $\pm 3.9 \times 10^{-10}$ | 42.28 ± 13.52 | 0.8449 ± 0.0123 | |
| 40 | 1.07 | 1.03×10^{-8} $\pm 3.2 \times 10^{-10}$ | 43.21 ± 12.19 | 0.8398 ± 0.0090 | |
| 60 | 1.07 | 1.03×10^{-8} $\pm 3.2 \times 10^{-10}$ | 43.28 ± 12.18 | 0.8399 ± 0.0090 | |
| 80 | 1.07 | 1.03×10^{-8} $\pm 3.2 \times 10^{-10}$ | 43.28 ± 12.18 | 0.8399 ± 0.0090 | |
| 100 | 1.07 | 1.03×10^{-8} $\pm 3.2 \times 10^{-10}$ | 43.28 ± 12.18 | 0.8399 ± 0.0090 | |
| ∞ | 1.07 | 1.03×10^{-8} $\pm 3.2 \times 10^{-10}$ | 43.28 ± 12.18 | 0.8399 ± 0.0090 | 0.209 $+0.012$ -0.014 |

For *n*-hexane, measurements were made at 38 different values of x^V in the range from 0.0001 to 0.90 at 20 °C.⁸ The value of the isotherm parameters and the value of $\Delta(\zeta)$ for a series of different values of ζ are listed in Table 2. Provided $\zeta \geq 40$, the error in the calculations is 0.68%. For $\zeta = 40$, the calculated amount adsorbed and the measurements are shown in Figure 2.

At 30 °C, Naono and Hakuman⁹ measured water vapor adsorption on silica (TK800) at 42 different values of x^V between 0.001 and 0.96. The values of the adsorption parameters for a series of different ζ values are listed in Table 3, along with values of $\Delta(\zeta)$. Provided $\zeta \geq 80$, the error in the calculated amount adsorbed is 0.54%. The measurements and the calculated amount adsorbed are shown in Figure 3. They also measured the water vapor adsorption on alumina (Baikowski CR1) at 26 different values of x^V between 0.008 and 0.931 at 20 °C. The values of the isotherm parameters are listed in Table 4, along with the corresponding values of $\Delta(\zeta)$. As seen there, provided $\zeta \geq 40$ the error in the calculations is less than 1.1%. Their

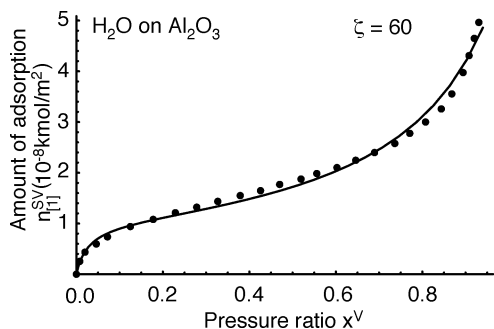


Figure 4. The solid dots indicate the measured amount of water vapor adsorbed on alumina (Baikowski CR1) at 20 °C.⁹ The solid line is the amount calculated from the ζ -isotherm relation when the maximum number of molecules in a cluster is 60. The other parameter values are listed in Table 4.

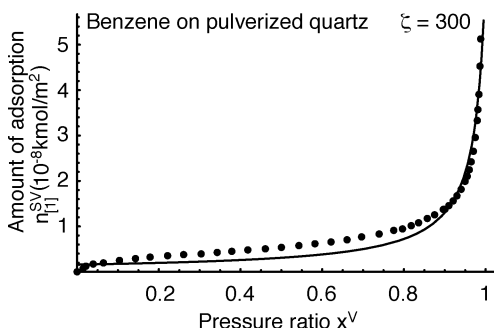


Figure 5. The solid dots indicate the measured amount of benzene adsorbed on quartz at 25 °C.¹⁰ The solid line is the amount calculated from the ζ -isotherm relation when the maximum number of molecules in a cluster is 300. The other parameter values are listed in Table 5.

TABLE 5: Parameters of the ζ -Isotherm for Benzene Adsorbing on Quartz at 25 °C Obtained from the Data of Naono, Hakuman, and Nakai¹⁰

| ζ | error, % | M (kmol/m ²) | c | α | $\gamma_{[1]}^{s0}$ (kg/s ²) |
|----------|----------|--|--------------------------------------|------------------------|--|
| 50 | 3.94 | 1.96×10^{-9} $\pm 3.5 \times 10^{-10}$ | 172.18 ± 1052.5 | 0.9782 ± 0.0188 | |
| 100 | 2.81 | 1.67×10^{-9} $\pm 1.4 \times 10^{-10}$ | 1857.95 $\pm 7.2 \times 10^{-11}$ | 0.9755 ± 0.0051 | |
| 150 | 2.56 | 1.62×10^{-9} $\pm 1.1 \times 10^{-10}$ | 8.29×10^{12} ± 0.0 | 0.9755 ± 0.0034 | |
| 200 | 2.50 | 1.59×10^{-9} $\pm 9.9 \times 10^{-11}$ | 3.36×10^{13} ± 0.0 | 0.9760 ± 0.0030 | |
| 300 | 2.49 | 1.58×10^{-9} $\pm 9.5 \times 10^{-11}$ | 1.39×10^{13} ± 0.0 | 0.9763 ± 0.0028 | |
| ∞ | 2.48 | 1.58×10^{-9} $\pm 9.5 \times 10^{-11}$ | 1.54×10^{13} ± 0.0 | 0.9763 ± 0.0028 | 0.162 +0.008 -0.006 |

measurements along with the calculated adsorption is shown in Figure 4. The surfaces of both silica (TK800) and alumina (Baikowski CR1) are polycrystalline; thus, the adsorption parameters would represent average values for the different crystallite planes that are exposed at the surface.

Naono, Hakuman, and Nakai¹⁰ reported the adsorption isotherm of benzene vapor on nonporous, pulverized quartz at 25 °C. They measured the amount of benzene vapor adsorbed at 45 different values of x^V between 0.014 and 0.99. The calculated values of the adsorption parameters and values of $\Delta(\zeta)$ are listed in Table 5. For $\zeta \geq 300$, $\Delta(\zeta)$ was less than 2.5%. In Figure 5 the measurements and the calculated amount adsorbed are shown. We note that of the five systems considered this is the largest error in the calculated amount adsorbed, and the largest inferred value of ζ . This suggests that the roughness of the pulverized quartz may have played a role in the measurements.

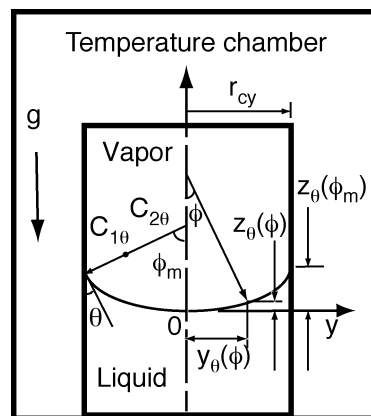


Figure 6. The definition of parameters used in predicting the liquid–vapor interface shape.

Note that for each system considered, there is a threshold value of ζ : as ζ is progressively increased, the error in the calculated amount adsorbed, $\Delta(\zeta)$, progressively decreases until the error reaches a minimum value, but the error does not diminish further (see Tables 1–5), even if ζ is allowed to approach infinity. Physically, this suggests that there are limited numbers of molecules in the clusters, and allowing more than the threshold value does not improve the accuracy of the calculated amount, perhaps because no clusters with a larger number of molecules are present. If ζ is allowed to be larger than the threshold value, the accuracy in the calculated amount adsorbed does not diminish. This allows the ζ -isotherm expression to be simplified without losing accuracy: thus, we take the limit of ζ approaching infinity, and use the corresponding values of M , c , and α in further calculations. This reduces eq 42 to eq 21.

2.5. Magnitude of $I_{\theta}(x_w^L, x_{\pi}^L)$ When the Pressure Is Such That a Contact Angle Exists. We now examine the magnitude of $I_{\theta}(x_w^L, x_{\pi}^L)$ that appears in eqs 17 and 20, and show this integral is negligible compared with γ^{LV} when the pressure is such that an equilibrium contact angle can exist. Since $x_3^L \leq x_{\pi}^L$ and $n_{[1]}^{SV}(x_3^V)$ are positive, an upper bound to $I_{\theta}(x_w^L, x_{\pi}^L)$ is provided by the integral $J(x_w^L, x_{\pi}^L)$:

$$J(x_w^L, x_{\pi}^L) \equiv \int_{x_w^L}^{x_{\pi}^L} n_{[1]}^{SV}(x_d^V) v_f P_s dx_d^L \quad (44)$$

$$I_{\theta}(x_w^L, x_{\pi}^L) \leq J(x_w^L, x_{\pi}^L) \quad (45)$$

The expression for $n_{[1]}^{SV}(x^V)$ is now available, but the values of x_w^L and x_{π}^L are yet to be determined. The three-phase system considered (see Figure 6) is one in which the liquid and vapor phases are held in a cylindrical container of radius r_{cy} , and exposed to a gravitational field of intensity g .

In Appendix A, the necessary conditions for equilibrium are used with the turning angle method to determine the values x_w^L and x_{π}^L as a function of T for an axi-symmetric liquid–vapor interface in cylinders of different radii, and the results are summarized in Figure 7. Note that $x_w^L < 1$, but $x_{\pi}^L > 1$; thus, the integral $J(x_w^L, x_{\pi}^L)$ in eq 44 would not be defined if isotherms such as the BET,¹¹ FHH,^{12–14} or AD¹⁵ were used, since each of them indicates an infinite amount adsorbed when x_3^L is unity, but, by contrast, the ζ -isotherm indicates a finite amount adsorbed under this condition. Also, it may be noted that the largest difference between x_w^L and x_{π}^L , for a given temperature, occurs for the smaller sized cylinders. This means the integral

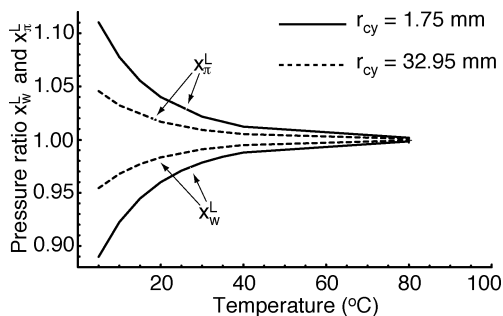


Figure 7. Values of the pressure ratio at the three-phase line in the liquid phase of water when θ is zero, and when θ is π for differently sized cylinders, and different temperatures.

TABLE 6: Values of $J(x_w^L, x_\pi^L)$ for Liquid–Vapor Systems in 0.56 mm Radii Cylinders

| | water–silica | benzene–carbon (basal plane) | <i>n</i> -hexane–carbon (basal plane) |
|------------------------------------|----------------------|---------------------------------|--|
| $T(^{\circ}\text{C})$ | 30 | 20 | 20 |
| x_w^L | 0.94013 | 0.98969 | 0.99577 |
| $1 - x_w^V$ | 2×10^{-6} | 4×10^{-6} | 4×10^{-6} |
| x_π^L | 1.05987 | 1.01031 | 1.00423 |
| J (kg/s ²) | 8.7×10^{-7} | 4.8×10^{-7} | 3.3×10^{-7} |
| γ^{LV} (kg/s ²) | 0.0712 | 0.0289 | 0.0184 |

$J(x_w^L, x_\pi^L)$ has its larger values for smaller sized cylinders. This allows a major simplification in evaluating $J(x_w^L, x_\pi^L)$: the Bond number ($Wgr_{cy}^2/v_f\gamma^{LV}$) decreases as the cylinder radius is reduced, and if the Bond number becomes small compared to unity, the interface may be approximated as spherical.²⁰

When the liquid–vapor interface is spherical, the curvatures are equal and constant along a liquid–vapor interface, but their value depends on θ . If the curvatures at a point on the interface when the contact angle is θ are denoted $C_{i\theta}(\phi)$, for $i = 1$ or 2 , then for a spherical interface

$$C_{1\theta}(\phi) = C_{2\theta}(\phi) = C_\theta \quad (46)$$

Geometry allows C_θ to be expressed

$$C_\theta = \frac{\cos \theta}{r_{cy}} \quad (47)$$

and $\cos \theta$ to be expressed (see Figure 6)

$$\cos \theta = \frac{2r_{cy}z_\theta(\phi_m)}{z_\theta(\phi_m)^2 + r_{cy}^2} \quad (48)$$

The expression for $J(x_w^L, x_\pi^L)$ can now be determined: from eq 12

$$dx_3^L = \frac{v_g dx_3^V}{v_f x_3^V} \quad (49)$$

and $J(x_w^L, x_\pi^L)$, given in eq 44, can be converted to an integral over x_3^V . One finds from eqs 21, 44, and 49

$$J(x_w^L, x_\pi^L) = MP_s v_g \ln \left(\frac{(-1 + \alpha x_w^V)[1 + (c-1)\alpha x_\pi^V]}{(-1 + \alpha x_\pi^V)[1 + (c-1)\alpha x_w^V]} \right) \quad (50)$$

A method is given in Appendix B by which $J(x_w^L, x_\pi^L)$ may be evaluated, and the results obtained for three different systems

are shown in Table 6. Note that in each case the $J(x_w^L, x_\pi^L)$ is 5 orders of magnitude smaller than γ^{LV} . Since $J(x_w^L, x_\pi^L)$ is larger than $I(x_w^L, x_\pi^L)$, the latter integral is completely negligible in eqs 17 and 20. Hence, provided the pressure is such that the contact angle can exist ($x_w^L \leq x_3^L \leq x_\pi^L$)

$$\gamma_{[1]}^{SV}(x_3^L) = \gamma^{LV} \quad (51)$$

and $\gamma_{[1]}^{SL}$ can be expressed in terms of the contact angle. From eq 20

$$\gamma_{[1]}^{SL}(x_3^L) = \gamma^{LV}[1 - \cos \theta(x_3^L)] \quad (52)$$

We note that at x_3^L equal x_w^L , eq 51 gives

$$\gamma_{[1]}^{SV}(x_w^L) = \gamma^{LV} \quad (53)$$

and this result is exact in the sense that no approximation is made to obtain it from the formulation (see eq 19); thus, the result indicates that in the pressure range considered, the adsorption at the solid–vapor interface is not strong enough to change $\gamma_{[1]}^{SV}$ from its value at wetting, but it is important to note that the pressure range is very small (see below).

By contrast, eq 52 indicates that $\gamma_{[1]}^{SL}(x_3^L)$ changes significantly in the pressure range considered, going from zero at wetting to $2\gamma^{LV}$ at x_π^L . The reason for this change in $\gamma_{[1]}^{SL}$ can be seen by integrating eq 10 subject to the condition given in eq 13:

$$\cos \theta(x_3^L) = \frac{v_f P_s}{\gamma^{LV}} \int_1^{x_3^L} [n_{[1]}^{SL}(x_d^L) - n_{[1]}^{SV}(x_d^L)] dx_d^L \quad (54)$$

Thus, the net adsorption at the three-phase line is seen to be the mechanism by which θ is changed as x_3^L is changed, and when eq 54 is compared with eq 52, this mechanism is seen to be the one that changes $\gamma_{[1]}^{SL}(x_3^L)$.

3. Expression for $\gamma^{SV}(x^V)$ When $x^V \leq x_w^V$: A Test of the Theory

When the pressure ratio is below x_w^V , equilibrium can no longer exist between the three phases, but only between the phase adsorbed on the solid surface and the vapor phase. The equilibrium conditions in eq 3 reduce to

$$\mu^V = \mu^{SV} \quad (55)$$

and from eqs 6 and 11, the Gibbs adsorption equation at the solid–vapor interface becomes

$$d\gamma_{[1]}^{SV}(x^V) = -n_{[1]}^{SV}(x^V) \frac{k_b T}{x^V} dx^V \quad (56)$$

If the expression for $n_{[1]}^{SV}$ given in eq 21 is combined with eq 56 and the result integrated from the wetting condition where $\gamma_{[1]}^{SV}$ has a value of γ^{LV} (see eq 53), one finds

$$\gamma_{[1]}^{SV}(x^V) = \gamma^{LV} + Mk_b T \ln \left(\frac{(1 - \alpha x^V)[1 + (c-1)\alpha x_w^V]}{(1 - \alpha x_w^V)[1 + (c-1)\alpha x^V]} \right) \quad (57)$$

The pressure ratio in the vapor at wetting, x_w^V , is very near unity for all the systems considered. As illustrated in Figure 7, the maximum deviation of x_w^L from unity occurs in the smaller sized cylinders at the lower temperatures, and as indicated in

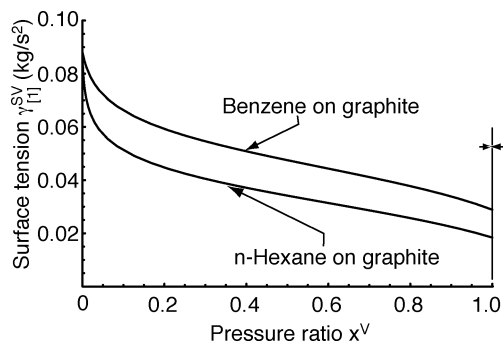


Figure 8. The calculated values of $\gamma_{[1]}^{SV}$ for the basal plane of carbon when exposed to benzene or *n*-hexane at pressure ratios less than x_w^V and a temperature of 20 °C. The pressure range over which the contact angle can exist is indicated by the vertical line near unity.

Table 6, the value of x_w^V in a 0.56 mm diameter capillary for water, benzene, and *n*-hexane deviates from unity by 4×10^{-6} or less. Thus, in eq 57 we approximate x_w^V as unity. Then, from eq 57:

$$\gamma_{[1]}^{SV}(x^V) = \gamma^{LV} - Mk_b T \ln \left(\frac{(\alpha - 1)[1 + (c - 1)\alpha x^V]}{(\alpha x^V - 1)[1 + (c - 1)\alpha]} \right) \quad (58)$$

The amount adsorbed decreases as x^V is decreased, and as seen in Figure 8, in the pressure range considered $\gamma_{[1]}^{SV}$ increases by a factor of more than 4 as x^V is decreased to zero. In view of eq 56, this can be understood as the effect on $\gamma_{[1]}^{SV}$ of decreasing the adsorption by lowering x^V .

When x^V is lowered to zero a special state is reached. From eq 58

$$\gamma_{[1]}^{S0} = \gamma^{LV} + Mk_b T \ln \left(1 + \frac{c\alpha}{1 - \alpha} \right) \quad (59)$$

The surface tension of a solid surface in the absence of adsorption, $\gamma_{[1]}^{S0}$, is a material property of the solid. Although the values of M , c , and α are determined by measuring the amount of vapor adsorbed on the solid surface, if the theory is valid eq 59 should define a material property. This interpretation can be tested for the basal plane of carbon, since measurements were reported of benzene and of *n*-hexane adsorbing on this surface at 20 °C.⁸ As seen in Figure 8, the values of $\gamma_{[1]}^{SV}$ obtained from adsorption measurements of benzene and those with *n*-hexane approach one another in the limit of x^V approaching zero. The value obtained for γ^{S0} in this limit from the study with benzene is listed in Table 1, and that obtained from the adsorption of *n*-hexane is listed in Table 2. The error bar is $\pm 3\%$ in the former case and $\pm 1\%$ in the latter, and the error bars overlap. Thus, there is no measurable difference between the values of $\gamma_{[1]}^{S0}$ determined by these two independent measurements. The error bars result from the error in the inferred values of M , c , and α . The agreement between the inferred values of $\gamma_{[1]}^{S0}$ from measurements with benzene and independently with *n*-hexane suggests eq 59 does, in fact, define a material property of a solid surface and the value obtained from the theory is independent of the vapor used to measure $\gamma_{[1]}^{S0}$.

This possibility may be examined further by considering the value of $\gamma_{[1]}^{S0}$ obtained for SiO₂ (TK800) at 30 °C and for quartz at 25 °C. The surfaces of both these materials consist primarily of SiO₂, but in the experiments, neither was a single-crystal surface.^{9,10} Nonetheless, one could reasonably expect the values of $\gamma_{[1]}^{S0}$ to be similar for the two materials, even though their

temperatures are slightly different. The value for SiO₂ (TK800) determined from the study with water vapor is listed in Table 3, and that for quartz determined from the study with benzene vapor is listed in Table 5. Their mean values differ by only 11%, and the one at the higher temperature has the lower value of $\gamma_{[1]}^{S0}$.

The fact that the values of $\gamma_{[1]}^{S0}$ calculated from measurements made by adsorbing different vapors on the same solid surface indicates the wetting hypothesis leads to consistent values of the $\gamma_{[1]}^{S0}$, and the proposed method can be used to determine the surface tensions.

4. Discussion and Conclusion

The results obtained are based on the Gibbs adsorption equations, the conditions for equilibrium, and an equilibrium adsorption isotherm at the solid–vapor interface. A new equation is obtained for an isothermal system that expresses $n_{[1]}^{SL}$ in terms $n_{[1]}^{SV}$ and θ (see eq 10). This eliminates the need to determine the expression for an adsorption isotherm at the solid–liquid interface. Both $\gamma_{[1]}^{SV}$ and $\gamma_{[1]}^{SL}$ are expressed in terms of an integral of $n_{[1]}^{SV}$ (see eqs 17, 18, and 20). Isotherms that indicate an infinite amount adsorbed when x^V is unity cannot be applied because the limits of the integral of $n_{[1]}^{SV}$ extend above and below x_3^V equal unity, and the integral would not converge if these isotherms were applied.

When the adsorbate is approximated as consisting of molecular clusters, each possibly containing different numbers of molecules, one finds the ζ -isotherm relation that has four parameters, M , c , α , and ζ (see eq 42), but ζ can be eliminated. The parameter α is usually assumed unity, but its deviation from unity is important. If its value were unity, the ζ -isotherm would also predict an infinite amount adsorbed at x_3^V equal unity. If the values of the parameters are chosen so as to give the best agreement between the predictions and the measurements for five different vapor–solid surfaces, the value of α is found to be significantly less than unity for each case (see Tables 1–5 and Figures 1–5). The error in the calculated amount adsorbed compared with that measured is less than 1.1% for four of the five systems and less than 2.5% for the other. Thus, there appears no reason to assume α has a value of unity.

Although adsorption effects have generally been neglected in previous efforts to determine the surface tension of a solid–fluid interface,⁵ we find the importance of adsorption depends on both the existing pressure and whether it is $\gamma_{[1]}^{SV}$ or $\gamma_{[1]}^{SL}$ that is being considered. If the wetting hypothesis is adopted, a numerical value may be assigned to solid–fluid surface tensions. This hypothesis assigns a value of zero to $\gamma_{[1]}^{SL}$ at wetting, where x^L is equal to x_w^L and θ is zero (see Figure 7). This assignment is similar to the procedure adopted in constructing tables for the properties of water, where the enthalpy of water at 273.16 K is assigned a value of zero, and enthalpies at other conditions are measured relative to this state.

In the narrow pressure range ($x_w \leq x_3^L \leq x_w^L$) where the contact angle can exist (see Figure 8), adsorption does not change the value of $\gamma_{[1]}^{SV}$ from the value it has at wetting, γ^{LV} (see eq 53). As may be seen from eq 54, an integral of the net adsorption at the three-phase line is the determining factor in the expression for θ , and $\gamma_{[1]}^{SL}$, as indicated by eq 52. Thus, adsorption strongly changes $\gamma_{[1]}^{SL}$, as x_3^L is changed in this pressure range, and, as a result θ is changed as well. The value of $\gamma_{[1]}^{SV}$ ranges from zero to twice γ^{LV} .

For pressures below x_w^L , the contact angle cannot exist, and there is only the possibility of equilibrium between the vapor and the phase adsorbed on the solid surface. The maximum value of $\gamma_{[1]}^{SV}$ occurs when x^V approaches zero (see Figure 8). As x^V increases from zero to x_w^V , $\gamma_{[1]}^{SV}$ decreases until it reaches γ^{LV} . There is no liquid phase in this pressure range, but when x^V increases above x_w^V , the liquid phase appears. The wetting hypothesis can be seen as assuming that just when the liquid phase appears, the $\gamma_{[1]}^{SL}$ is zero. If this were not true, there would be a discontinuity in $\gamma_{[1]}^{SL}$ at x_w^V . For values $x_w^V \leq x^V \leq x_\pi^V$, the contact angle can exist. From this point of view, when adsorption has lowered $\gamma_{[1]}^{SV}$ from its maximum value, γ^{S0} , to γ^{LV} , there is no longer any potential for adsorption at the solid–vapor interface, but there is potential for adsorption at the solid–liquid interface, since this phase did not exist for $x^L < x_w^L$. As x^L is increased, in this narrow pressure range, $\gamma_{[1]}^{SL}$ changes markedly.

The proposed theory is testable. When x^V is too small for the contact angle to exist, $\gamma_{[1]}^{SV}$ can be expressed in terms of the adsorption isotherm parameters, M , c , α , and γ^{LV} (see eq 57), and as the independent variable x^V . When this relation is evaluated at $x^V = 0$, an expression for $\gamma_{[1]}^{S0}$, a material property of the solid surface, is obtained. An important test of the theory is then possible because this material property can be determined by adsorbing different vapors in independent experiments on the same solid surface. The value of $\gamma_{[1]}^{S0}$ should be the same in each case. This procedure was used to determine $\gamma_{[1]}^{S0}$ for graphitized carbon from adsorption measurements made with benzene and with *n*-hexane at 20 °C. The mean values of $\gamma_{[1]}^{S0}$ were different by 3%, but the error bars overlapped. So there was no measurable difference between the values of $\gamma_{[1]}^{S0}$ (see Figure 8). The theory is further supported by the results found for quartz and silica (TK800). Although the surfaces of each of these materials are polycrystalline, each consists primarily of SiO₂. Thus, one would expect $\gamma_{[1]}^{S0}$ for each surface to have similar values. The values obtained are listed in Tables 3 and 5. Note the mean value for silica (TK800) at 30 °C is 11% smaller than that of quartz at 25 °C.

Acknowledgment. This work was supported by the Natural Sciences and Engineering Research Council of Canada.

Appendix A: Determination of x_w^L or x_π^L

The liquid–vapor interface of the system shown schematically in Figure 6 is axi-symmetric, and when x_3^L has the value x_w^L or x_π^L , the values of θ are, by definition, zero and π , respectively. When combined with the necessary conditions for equilibrium, this is sufficient information to determine the values of x_w^L or x_π^L .

One of the conditions for equilibrium may be written^{1,3}

$$\mu^j + Wgz = \lambda \quad (60)$$

where λ is a constant. A second condition for equilibrium is the Laplace equation. If the curvatures at a point on the liquid–vapor interface are denoted $C_{1\theta}(\phi)$ and $C_{2\theta}(\phi)$ when a contact angle θ exists at the three-phase line, and a radius of curvature is taken as positive when the vapor is inside the surface, the Laplace equation may be written (see Figure 6)

$$C_{1\theta}(\phi) + C_{2\theta}(\phi) = \frac{P_s}{\gamma^{LV}} \left[\exp\left(\frac{v_f}{v_g} [x_\theta^L(\phi) - 1]\right) - x_\theta^L(\phi) \right] \quad (61)$$

where we have made use of eq 12. The curvature $C_{2\theta}(\phi)$ is related to the radial position on the interface $y_\theta(\phi)$ by

$$C_{2\theta}(\phi) = \frac{\sin \phi}{y_\theta(\phi)} \quad (62)$$

On the longitudinal axis of symmetry, $C_{1\theta}$ and $C_{2\theta}$ are equal, and are denoted $C_\theta(0)$. When eq 61 is applied on the axis of symmetry, it reduces to

$$C_\theta(0) = \frac{P_s}{2\gamma^{LV}} \left[\exp\left(\frac{v_f}{v_g} [x_\theta^L(0) - 1]\right) - x_\theta^L(0) \right] \quad (63)$$

After combining eqs 4 and 60, and applying the result at the point where the liquid–vapor interface crosses the axis of symmetry (i.e., the coordinate system origin, see Figure 6) and at an arbitrary position on the liquid–vapor interface, one finds

$$x_\theta^L(\phi) = x_\theta^L(0) - \frac{Wgz_\theta(\phi)}{v_f P_s} \quad (64)$$

Since $z_\theta(\phi)$ is measured from the coordinate system origin, it is positive if the vapor is inside the surface of curvature, but negative when the vapor is outside the surface of curvature.

The expression for $C_{1\theta}(\phi)$ may be obtained from eqs 12 and 61–64:

$$C_{1\theta}(\phi) = \frac{P_s x_\theta^L(0)}{\gamma^{LV}} \left(\exp\left[-\frac{Wgz_\theta(\phi)}{P_s v_g}\right] - 1 \right) + 2C_\theta(0) - \frac{\sin \phi}{y_\theta(\phi)} + \frac{Wgz_\theta(\phi)}{\gamma^{LV} v_f} \quad (65)$$

and from differential geometry

$$\frac{dy_\theta(\phi)}{d\phi} = \frac{\cos \phi}{C_{1\theta}(\phi)} \quad (66)$$

$$\frac{dz_\theta(\phi)}{d\phi} = \frac{\sin \phi}{C_{1\theta}(\phi)} \quad (67)$$

When the contact angle is zero or π , the maximum value of the turning angle, ϕ_m , is $\pi/2$ in both cases. However, in the former case the three-phase line is above the origin and $z_w(\phi)$ is positive, but in the latter, the three-phase line is below the origin and $z_\pi(\phi)$ is negative. The boundary condition that the solution to eqs 65–67 must satisfy is the same

$$y_w(\pi/2) = y_\pi(\pi/2) = r_{cy} \quad (68)$$

but there is a change in the sign of z in the governing equations between the two cases.

From eq 64, the pressure ratio at the three-phase line when the contact angle is θ , $x_\theta^L(\phi_m)$, may be expressed

$$x_\theta^L(\pi/2) = x_\theta^L(0) - \frac{Wgz_\theta(\pi/2)}{v_f P_s} \quad (69)$$

We consider an iterative method to determine the solution of eqs 65–67: a value of $C_\theta(0)$ is assumed, and the corresponding value of $x_\theta^L(0)$ is determined from eq 63. The expression for $C_{1\theta}(\phi, C_\theta(0))$ can then be determined from eq 65, and used in eqs 67 and 68. The result is integrated over the range

$$0 \leq \phi \leq \pi/2 \quad (70)$$

If the correct value of $C_\theta(0)$ has been chosen, then the calculated value of $y_\theta(\pi/2; C_\theta(0))$ will be equal to r_{cy} . If not, then another value of $C_\theta(0)$ is chosen, and the process repeated until the boundary condition is satisfied. The values of x_w^L and x_π^L obtained from this procedure are shown in Figure 7 for different temperatures and cylinders of different radii.

Appendix B: Values of x_w^V and x_π^V

For a particular vapor–liquid–solid system, the integral $J(x_w^L, x_\pi^L)$ may be evaluated once the values of x_w^V and x_π^V have been determined. We first express x_w^V and x_π^V in terms of pressure ratios in the liquid phase at the three-phase lines. Three steps are required. From eq 12

$$x_w^V(\phi) = \exp\left(\frac{v_f}{v_g}[x_w^L(\phi) - 1]\right) \quad (71)$$

and

$$x_\pi^V(\phi) = \exp\left(\frac{v_f}{v_g}[x_\pi^L(\phi) - 1]\right) \quad (72)$$

Second, $x_w^L(\phi)$ and $x_\pi^L(\phi)$ are written in terms of the pressure ratio on the axis of symmetry of the cylinder when the contact angle is zero, $x_w^L(0)$, and when it is π , $x_\pi^L(0)$. When θ has a value of zero, one finds from eq 48 that $z(\pi/2)$ has a value of r_{cy} , and then from eq 64

$$x_w^L(\pi/2) = x_w^L(0) - \frac{Wgr_{cy}}{v_f} \quad (73)$$

and if θ has a value of π , $z(\pi/2)$ has a value of $-r_{cy}$, and eq 64 gives

$$x_\pi^L(\pi/2) = x_\pi^L(0) + \frac{Wgr_{cy}}{v_f} \quad (74)$$

Finally, an equation to establish the values of $x_w^L(0)$ and $x_\pi^L(0)$ is obtained by combining eqs 61, 46, and 47, and evaluating

the result when both θ and ϕ are zero:

$$\exp\left(\frac{v_f}{v_g}[x_\theta^L(0) - 1]\right) - x_\theta^L(0) = \frac{2\gamma^{LV}}{r_{cy}P_s} \quad (75)$$

For given values of T , r_{cy} , the isotherm parameters (M , c , and α), and the fluid properties, eqs 71–75 constitute a closed system of equations that can be applied to calculate the values of x_w^V and x_π^V . These values may then be used in eq 50 to determine the value of $J(x_w^L, x_\pi^L)$. The results obtained for three different systems are listed in Table 6.

References and Notes

- (1) Gibbs, J. W. *Trans. Conn. Acad. Arts Sci.* **1876**, 3, 108; republished as *The Scientific Papers of J. Willard Gibbs*; Bumstead, H. A., Van Name, R. G., Eds.; Dover: New York, 1961; Vol. 1, p 219.
- (2) Johnson, R. E. *J. Phys. Chem.* **1959**, 63, 1655.
- (3) Ward, C. A.; Sages, M. R. *J. Chem. Phys.* **1998**, 109, 3651.
- (4) Graf, K.; Riegler, H. *Langmuir* **2000**, 16, 5187.
- (5) Chibowski, E.; Perea-Carpio, R. *Adv. Colloid Interface Sci.* **2002**, 98, 245.
- (6) Frazer, J. H. *Phys. Rev.* **1929**, 33, 97.
- (7) Anderson, R. B. *J. Am. Chem. Soc.* **1946**, 68, 686.
- (8) Isirikyan, A. A.; Kiselev, A. V. *J. Phys. Chem.* **1961**, 65, 601.
- (9) Naono, H.; Hakuman, M. *J. Colloid Interface Sci.* **1991**, 145, 405.
- (10) Naono, H.; Hakuman, M.; Nakai, K. *J. Colloid Interface Sci.* **1994**, 165, 532.
- (11) Brunauer, S.; Emmett, P. H.; Teller, E. *J. Am. Chem. Soc.* **1938**, 60, 309.
- (12) Frenkel, Y. I. *Kinetic Theory of Liquids*; Clarendon Press: Oxford, UK, 1946; p 308.
- (13) Halsey, G. *J. Chem. Phys.* **1948**, 16, 931.
- (14) Hill, T. L. In *Advances in Catalysis and Related Subjects*; Frankenburg, W. G., Komarewsky, V. I., Rideal, E. K., Eds.; Academic Press: New York, 1952; Vol. 4, p 211.
- (15) Aranovich, G. L.; Donohue, M. D. *J. Colloid Interface Sci.* **1995**, 173, 515.
- (16) Hill, T. L. *Introduction to statistical thermodynamics*; Addison Wesley: New York, 1960; p 134.
- (17) Polley, M. H.; Schaeffer, W. D.; Smith, W. R. *J. Phys. Chem.* **1953**, 57, 469.
- (18) Avgul, N. N.; Kiselev, A. V. In *Chemistry and Physics of Carbon*; Walker, P. L., Jr., Ed.; Marcel Dekker Inc.: New York, 1970; Vol. 6, p 1.
- (19) Spencer, W. B.; Amberg, C. H.; Beebe, R. A. *J. Phys. Chem.* **1958**, 62, 719.
- (20) Sages, M. R.; Ward, C. A.; Azuma, H.; Yoshihara, S. *J. Appl. Phys.* **1996**, 79, 8770.